2021 43rd Annual International Conference of the
IEEE Engineering in Medicine & Biology Society (EMBC)
Oct 31 - Nov 4, 2021. Virtual Conference

A Compartmental Model for the Iron Trafficking Across the Blood-Brain Barriers in Neurodegenerative Diseases

E. Ficiarà, F. D'Agata, S. Cattaldo, L.Priano, A. Mauro and C. Guiot

Abstract – **Iron accumulation in the brain is supposed to play a central role in the induction of oxidative stress and consequently in neurodegeneration. The sensitive balance of iron in the brain is maintained by the brain barriers system, i.e., the blood-brain barrier between the blood and brain interstitial fluid and the blood-cerebrospinal fluid barrier between the blood and cerebrospinal fluid (CSF). In this work, we proposed a three-compartmental mathematical model simulating iron trafficking between blood, CSF, and cerebral space, describing the direction of fluxes based on the structural and functional characteristics of the brain barriers system. Different techniques of sensitivity analysis were used to evaluate the most important parameters, providing an indication for the most relevant biological functions that potentially affect the physiological transport of iron across brain barriers.**

I. Introduction

Iron is a critical element for most organisms, fundamental in several physiological processes. Its biological role is attributable to its oxido-reductive properties, which make iron essential but also cause toxicity, in the case of free ions concentration runs out of control.

Consequently, the disruption of iron homeostasis has severe impacts on the brain, being particularly sensitive to such modifications. Brain iron accumulation is assumed to have a central role in neurodegeneration by inducing oxidative stress [1]. Iron homeostasis in the brain is dynamically maintained by the brain barriers system separating blood and cerebral space. Imbalance of iron metabolism is involved in several neurodegenerative disorders, such as Alzheimer's Disease (AD) and dementia, leading to iron overload and dysfunction of iron-related proteins [2]. The iron balance of the brain depends both on iron influx and efflux rates, and throughout life, their changes reflect the change in the brain iron dynamics. Interestingly, the rate of iron accumulation depends on aging [3] and the relative imbalance of influx and efflux rate is involved in neurodegeneration. However, the understanding of the mechanisms of brain iron import/export is still limited, requiring further investigation.

It is reported that metals such as iron and copper may enter the interstitial fluid of the brain via the blood-brain barrier (BBB), be transported back into the blood via the efflux mechanism at the blood-cerebrospinal fluid barrier (BCSFB), known to remove substances from the cerebrospinal fluid (CSF) to the blood [4]. Since there is no structural barrier between the CSF and interstitial fluid (ISF), materials in these two fluids compartments can freely exchange, in a bidirectional way [5].

Mathematical models are useful tools to simulate the biological dynamic of a system and the complex networks of its components. The accuracy of results from mathematical models of biological systems is often perturbed by the presence of uncertainties in experimental data. Sensitivity analysis (SA) quantifies uncertainty, assessing how variations in model outputs can be apportioned, qualitatively or quantitatively, to different input sources. Many techniques have been developed to investigate multi-dimensional parameter spaces [6].

Based on our previous study [7], this work aims to implement a more complete mathematical model, able to describe macroscopically the iron exchange at the blood-brain interface, considering the functional role of the brain barriers. Numerical simulations and global SA are performed to investigate the behavior of the system and how the most relevant parameters can affect brain iron regulation.

II. Material and Methods

A. Mathematical Model

A three-compartmental model (see Figure 1) based on a non-homogeneous system of first-order ordinary differential equations (ODEs), described by (1), (2), and (3), is proposed to study the passage of iron from blood to brain. The parameters and variables entering the equations are listed below.

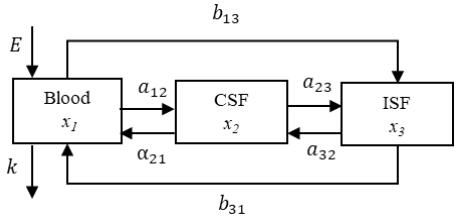

Figure 1. Schematic representation of the barriers forming blood-brain interface, considering blood, CSF and ISF as the three compartments in which the iron concentrations x_1, x_2, x_3 are modulated by the constant E and the parameters listed below.

$$\begin{cases} \frac{dx_1}{d\tau} = -(a_{12}+k)x_1 + a_{21}x_2 - b_{13}x_1 + b_{31}x_3 + E & (1) \\ \frac{dx_2}{d\tau} = a_{12}x_1 - (a_{21}+a_{23})x_2 + a_{32}x_3 & (2) \\ \frac{dx_3}{d\tau} = b_{13}x_1 + a_{23}x_2 - (a_{32}+b_{31})x_3 & (3) \end{cases}$$

*Research supported by the University of Turin (RiLo to CG).

E.F., F.D.A., L.P., A.M. and C.G. authors are with the Department of Neurosciences at the University of Torino, Torino, Italy (corresponding author, e-mail: eleonora.ficiara@unito.it)

S.C., L.P., and A.M. are with Istituto Auxologico Italiano, IRCCS, Laboratory of Clinical Neurobiology, San Giuseppe Hospital, Verbania, Italy.

We defined $\tau = t/T$ (T=1 day, timescale for normalization) and replaced $t = T \cdot \tau$ in to obtain rate constants as adimensional quantities.

The values of the parameters k, a_{12} and the constant E have been estimated as described in our previous model [7]. In this model, four parameters (a_{23}, a_{32}, b_{13}, b_{31}) were added to account for the exchange of iron to the third compartment (ISF), and one parameter was modified with respect to the two-compartmental model (α_{21} replaced to a_{21}). The proposed values for these new parameters were estimated taking into account data for iron concentrations, exchange, and the description of the biological structure of brain barriers present in the literature [4,8,9,10,11,12]. The terms entering the equations (1), (2), and (3) are listed below:

- x_1: Iron concentration in blood (mg/L);
- x_2: Iron concentration in CSF (mg/L);
- x_3: Iron concentration in ISF (mg/L);
- E: Iron intake into the blood from food (mg/L); fixed quantity;
- k: Iron consumption from blood and excretion mechanisms;
- a_{12}: Kinetic constant rate for iron entering from blood to CSF across BCSFB;
- α_{21}: Kinetic constant rate for iron returning from CSF and brain to blood;
- a_{23}: Kinetic constant rate for iron passing from CSF to ISF;
- a_{32}: Kinetic constant rate for iron passing from ISF to CSF;
- b_{13}: Kinetic constant rate for iron entering from blood to brain (consequently ISF), across BBB;
- b_{31}: Kinetic constant rate for iron returning from the brain to blood.

B. Numerical Simulations and Stability Analysis

Numerical simulations of the ODEs system were performed, setting x_{10}, x_{20}, and x_{30} as initial conditions and the value of parameters according to Table I (see Results).

Phase-plane analysis was pursued in order to investigate the system near an equilibrium point and how the most relevant parameters affect the dynamic of the system. The values of the steady state for each variable (x_{1s},x_{2s},x_{3s}) reported in Appendix were obtained by solving the system of ODEs described by (1), (2), and (3) setting the term $\frac{dx_i}{dt}$ =0 (i=1,2,3).

C. Sensitivity Analysis

We used different methods to perform global SA to evaluate the overall effects of the perturbations of the model input, and thus to rank these parameters according to their influence on the model output. Firstly, we used the Morris method [13] to screen the variables and to obtain a qualitative sensitivity measure. The average of the elementary effects (μ*) quantifies the importance of the parameters for the model output, while the standard deviation of the elementary effects (σ) indicates the non-linear effect of the model parameters on the output. Then, we applied the variance-based Sobol method, returning the first- and second-order sensitivity indices and total effect sensitivity index [14,15]. We evaluated the results of Morris analysis and Sobol indices for the concentration of iron in blood x_1, in the CSF x_2 and in ISF x_3. 15000 samples of model inputs were generated based on Morris method for sampling. For the Sobol method, 15000 samples were generated by means of Saltelli's sampling scheme. Bounds of input parameters range were set accordingly to cover the different values of the parameters, assuming physiological and pathophysiological conditions. The Sobol index threshold for sensitive input parameters was 0.01. SALib library of Python was used to perform SA [16].

III. Results

A. Numerical Simulations

We performed numerical simulations of the three-compartmental model described by equations (1), (2), and (3). By expressing the iron concentrations in blood, CSF, and ISF in mg/L, we set the constant E=0.22, k=0.23 and the parameters values according to Table I, assuming different sets of initial conditions (i.e., reflecting possible biological state: concentration of ISF>CSF, CSF>ISF, and concentration of CFS and ISF comparable). We focused on the concentration of iron in the cerebral space, so we reported the results for iron in CSF and ISF, showing the time course of the system for different rates of exchange (Figure 2, Figure 3). As expected, the rate of iron income to the brain is much lower from blood and ISF due to the presence of the BBB, while iron returns to blood mainly via CSF.

TABLE I. VALUES OF THE PARAMETERS OF THE MODEL (a_{12}, α_{21} , a_{23} , a_{32}, b_{13} , b_{31})

Parameter	Physiological Condition	High Rate Condition
a_{12}	$2 \cdot 10^{-4}$	0.001
α_{21}	0.05	0.08
a_{23}	0.8	0.8
a_{32}	1	1
b_{13}	0.002	0.005
b_{31}	$1 \cdot 10^{-6}$	$5 \cdot 10^{-6}$

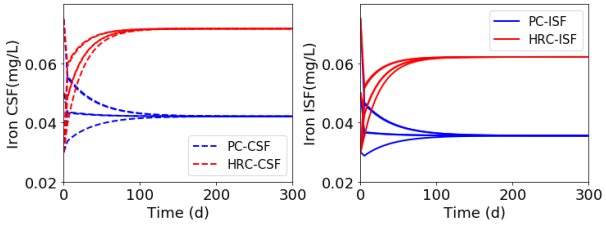

Figure 2. Simulations of the iron concentration in CSF and ISF for physiological condition (PC), and high-rate condition (HRC). Different combinations of initial conditions: x_{10} = 1 mg/L; x_{20} = 0.03;0.05;0.075 mg/L; and x_{30} = 0.03;0.05;0.075 mg/L. Parameters as referred in Table I; d=days.

Finally, we proposed a simulation for the condition of reduced clearance (Figure 3) from CSF (α_{21}=0.05, a_{32}=0.8) in presence of a high rate, being a possible pathobiological situation in neurodegenerative diseases.

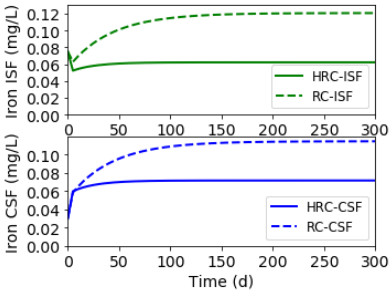

Figure 3. Simulations of iron concentration in CSF and ISF for high-rate condition (HRC) and hypothesis of condition of reduced clearance (RC). Initial conditions: x_{10} = 1 mg/L; x_{20} = 0.03 mg/L; and x_{30} = 0.075 mg/L. Parameters as referred in Table I; d=days.

Starting from 30 random initial conditions for the blood, ISF, and CSF we reported phase-plane for concentration of iron in CSF against ISF, and iron in blood against ISF (Figure 4).

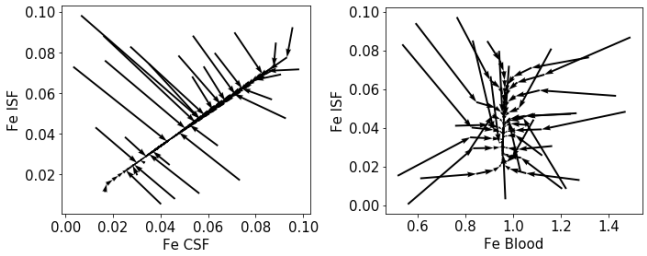

Figure 4. Phase-plane analysis for iron in CSF against ISF in the left, and for iron in blood against ISF in the right. Iron concentration are expressed in mg/L.

B. *Sensitivity Analysis*

Sensitivity analysis determined how much of the variability in model output (x_1,x_2,x_3) is dependent upon each of the input parameters (k, E, a_{12}, α_{21}, a_{23}, a_{32}, b_{13}, b_{31}). Based on our previous results on iron concentration in CSF and blood [7], we proposed a variation from initial conditions of 30% for the physiologic condition, and of 50% for the pathological one. The ranges of variations of the parameters for the pathological condition were assumed to be the following: for a_{12} [$2\cdot10^{-5}$: $2\cdot10^{-3}$], for α_{21} [0.005 : 0.4], for b_{13} [0.0002: 0.01], and for b_{31} [$8\cdot10^{-7}$: $5\cdot10^{-6}$]. We considered a restriction to half of each interval for the physiological condition. In both cases, the variation of the remaining parameters (k, E, a_{23}, a_{32}) is fixed to 20%.

Results from Morris analysis showed the four most relevant parameters affecting iron concentration in CSF and ISF, reported in Figure 5. Accordingly, the parameters α_{21} and b_{13} were the most important for CSF iron, especially in the pathological conditions. We found that the parameters E, a_{23}, a_{32}, b_{13} (especially b_{13}) mainly affect ISF iron, and α_{21} became relevant only in the pathological condition.

After screening the parameters by Morris method, Sobol analysis confirmed the previous results, showing that the parameters α_{21} and b_{13} were the most relevant for CSF iron (Figure 6).

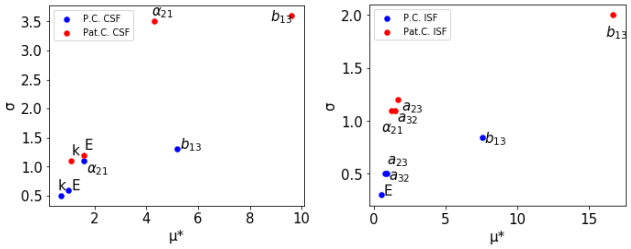

Figure 5. Plot of average elementary effects μ* against standard deviation σ of the most relevant parameters for iron concentration in CSF (left) and in ISF (right), considering physiological (P.C.) and pathological condition (Pat.C.). Both μ* and σ are adimensional.

In particular, α_{21} was more important for modulating iron in CSF in pathological with respect to physiological condition and became relevant ($S_1 > 0.01$) for ISF only in pathological condition. We reported the significant values obtained for the first-order Sobol index for CSF (x_2) and ISF iron concentration (x_3) (Figure 6).

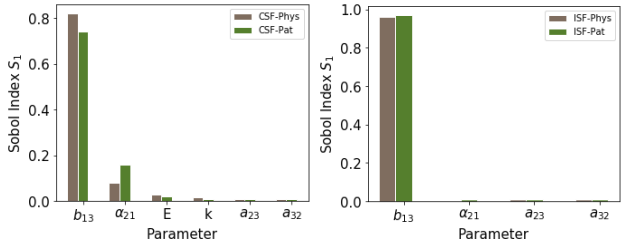

Figure 6. Bar plots of the first-order Sobol index S_1, for iron concentration in CSF (left) and ISF (right), showing the higher contribution of b_{13}.

Furthermore, the interactions of the two parameters regulating the barrier exchange, i.e., b_{13} and α_{21}, showed the strongest impact on the variability of iron concentration in CSF, reporting a significant value of the second-order index both in physiological (S_2 = 0.02 ± 0.01) and pathological condition (S_2 = 0.04 ± 0.02).

IV. Discussion and Conclusion

In this work we improved our previous model [7], proposing a three-compartmental model based on ODEs to macroscopically describe the iron exchange across the blood-brain barriers. Numerical simulations were performed in two conditions (Table I), being the high-rate condition supposed to be a consequence of the potential damage of the BBB causing higher exchange rates of iron. In both cases (Figure 2) the system reached a stable condition, showing that even starting from different initial conditions for ISF and CSF iron concentration, CSF stabilizes at larger concentration levels, potentially reflecting its biological function of "sink" for the removal of substances (i.e., redox-active metals) from ISF. Also, the condition of reduced clearance can reflect the pathobiological situation of altered removal mechanism from CSF and brain (Figure 3).

Phase-plane analysis suggested a possible correlation between the concentration of iron in CSF and ISF. Figure 4 underlines how iron content in CSF and ISF are linearly correlated (as expected in the absence of a selective barrier)

while the relationship between iron in ISF and blood is highly non-linear due to the presence of the barriers. The CSF status (in which are dosed biomarkers for neurodegeneration) reflects that of the brain while iron content in blood is highly non-linearly related to that in ISF, indicating iron biomarkers dosed in CSF might be more suitable than blood ones. Also, the system converged to stable solutions starting from different initial conditions of ISF, CSF, and blood (Figure 4).

For the SA, we considered the range of parameters in the pathological condition as possibly reflecting the damage of BBB (i.e., breakdown or leakage are common in neurodegeneration, as reported in the literature [17]). Morris analysis revealed that parameters α_{21} and b_{13} are the most relevant for the modulation of iron in CSF, and b_{13} showed the higher contribution (highest μ* and σ) for iron ISF in the pathological condition (Figure 5). The high value of σ in pathological condition could reflect non-linear effects on the iron concentration due to variations of this parameter. These results were confirmed by Sobol analysis (Figure 6) and could be considered in agreement with the evidence that iron from blood circulation is primarily transported to the brain parenchyma by the BBB [4].

The parameter α_{21} became relevant to explain iron in ISF in pathological conditions (both in Morris and in Sobol method), suggesting the importance of efflux rate mechanism of iron, controlled by bulk CSF flow and/or by the removal mechanism in the BCSFB back to the blood circulation [4,10]. This interesting result (and also the parameter a_{32}) could reflect the role of the 'glymphatic' system. This is a network of perivascular pathways supporting exchanges between CSF and ISF and contributing to the efflux of interstitial solutes (i.e., the toxic amyloid β, hallmark of AD) [18]. However, our model needs to be supported by ad-hoc experimental data for a more realistic and accurate estimation of the parameters and further refined, i.e., considering the time dependence of the parameters and the quantification of iron in the brain tissues.

In conclusion, simulating the regulation of iron homeostasis in the CNS and imbalance of influx/efflux rates in pathological condition by means of computational models can support both diagnostic and therapeutic innovations. In the last years, new treatments targeting the mechanisms at the brain barriers were of great interest driving to novel therapeutic strategies, and could be useful to counteract metal imbalance (e.g., chelation therapy) in neurodegenerative diseases.

APPENDIX

The expression of steady state for x_1, x_2 and x_3 were found as described in Methods.

$$x_{1s} = \frac{E}{k}$$

$$x_{2s} = \frac{E \cdot (a_{12} \cdot a_{32} + a_{12} \cdot b_{31} + a_{32} \cdot b_{13})}{C}$$

$$x_{3s} = \frac{E \cdot (a_{12} \cdot a_{23} + b_{13} \cdot a_{23} + \alpha_{21} \cdot b_{13})}{C}$$

Where C is defined as below.

$$C = a_{23} \cdot b_{31} \cdot k + a_{32} \cdot \alpha_{21} \cdot k + \alpha_{21} \cdot b_{31} \cdot k$$

REFERENCES

[1] A. Carocci, A. Catalano, M.S. Sinicropi, G. Genchi. "Oxidative stress and neurodegeneration: the involvement of iron." *Biometals* 31, 715–735 (2018)

[2] R.J. Ward, F.A. Zucca, J.H. Duyn, R.R. Crichton, L. Zecca. "The role of iron in brain ageing and neurodegenerative disorders", *Lancet Neurol* 13(10):1045-60 (2014)

[3] G. P. Holmes-Hampton, M. Chakrabarti, A. L. Cockrell, S. P. McCormick, L. C. Abbott, L. S. Lindahl and P. A. Lindahl "Changing iron content of the mouse brain during development" *Metallomics,* 4, 761–770, (2012)

[4] W. Zheng and A.D. Monnot "Regulation of Brain Iron and Copper Homeostasis by Brain Barrier Systems: Implication in Neurodegenerative Diseases" *Pharmacol Ther.* 133(2): 177–188 (2012)

[5] M. Matsumase, O. Sato, A Hirayama, N. Hayashi, K. Takizawa, H. Atsumi and T. Sorimachi "Research into the Physiology of Cerebrospinal Fluid Reaches a New Horizon: Intimate Exchange between Cerebrospinal Fluid and Interstitial Fluid May Contribute to Maintenance of Homeostasis in the Central Nervous System" *Neurol Med Chir (Tokyo)* 56(7): 416-41 (2016)

[6] S. Marino, I.B. Hogue, C.J. Ray, and D. E. Kirschner "A Methodology For Performing Global Uncertainty And Sensitivity Analysis In Systems Biology" *J Theor Biol.* 254(1): 178–196 (2008)

[7] E. Ficiarà, F. D'Agata, S. Ansari, S. Boschi, I. Rainero, L. Priano, S. Cattaldo, O. Abollino, R. Cavalli and C. Guiot "A mathematical model for the evaluation of iron transport across the blood-cerebrospinal fluid barrier in neurodegenerative diseases" *42nd Ann. Int. Conf. IEEE EMBC* (2020)

[8] E. Ficiarà, S. Boschi, S. Ansari, F. D'Agata, O. Abollino, P. Caroppo, G. Di Fede, A. Indaco, I. Rainero and C. Guiot "Machine Learning Profiling of Alzheimer's Disease Patients Based on Current Cerebrospinal Fluid Markers and Iron Content in Biofluids" Front. Aging Neurosci. 13:607858 (2021)

[9] I. Khan, J. Liu, and P. Dutta "Iron transport kinetics through blood-brain barrier endothelial cells" *Biochimica et Biophysica Acta (BBA)* 1862(5): 1168-1179 (2018)

[10] M.W. Bradbury "Transport of iron in the blood-brain-cerebrospinal fluid system." *J Neurochem.* 69(2):443-54 (1997)

[11] T. Lopes, T.Luganskaja, M.Spasic, M. Hentze, M. Muckenthaler, K. Schumann, J. Reich "Systems analysis of iron metabolism: the network of iron pool and fluxes" *BMC Systems Biology* 4:112 (2010)

[12] J. Chen, N. Singh, H. Taya and T. Walczyk "Imbalance of iron influx and efflux causes brain iron accumulation over time in the healthy adult rat" *Metallomics*, 6, 1417 (2014)

[13] M.D. Morris "Factorial Sampling Plans for Preliminary Computational Experiments" *Technometrics* 33(2): 161-174 (1991)

[14] I. M. Sobol, "Global sensitivity indices for nonlinear mathematical models and their Monte Carlo estimates." *Mathematics and Computers in Simulation*, 55(1-3): 271-280 (2001)

[15] A. Saltelli, P. Annoni, I. Azzini, F. Campolongo, M. Ratto, and S. Tarantola "Variance based sensitivity analysis of model output. Design and estimator for the total sensitivity index." *Computer Physics Communications* 181(2): 259-270 (2010)

[16] J. Herman and W. Usher "SALib: An open-source Python library for Sensitivity Analysis" *The Journal of Open Source Software* (2017)

[17] M. D. Sweeney, Z. Zhao, A. Montagne, A.R. Nelson, and B. V. Zlokovic "Blood-Brain Barrier: from Physiology to Disease and Back" *Physiological Reviews* 99: 21–78 (2019)

[18] J. Iliff and M. Simon "CrossTalk proposal: The glymphatic system supports convective exchange of cerebrospinal fluid and brain interstitial fluid that is mediated by perivascular aquaporin-4" *The Journal of Physiology* 597(17): 4417-4419 (2019)